ELSEVIER

Journal of Organometallic Chemistry 623 (2001) 191–201

Journal of Organometallic Chemistry

www.elsevier.nl/locate/jorganchem

Synthesis and characterization of new thioether derivatives of $[Os_3(CO)_{12}]$ and $[H_2Os_3(CO)_{10}]$; crystal and molecular structures of $[Os_3(CO)_{11}(L)]$ [Et_2S, Pr_2S, $S(CH_2)_5$] and $[Os_3(CO)_9(\mu\text{-}H)(\mu\text{-}X)\{SMe(Bu^t)\}]$ (X = H, OH)

Nitsa K. Kiriakidou-Kazemifar [a], Eike Kretzschmar [a,1], Håkan Carlsson [a], Magda Monari [b], Simona Selva [b], Ebbe Nordlander [a,*]

[a] *Inorganic Chemistry 1, Chemical Center, Lund University, Box 124, S-22100 Lund, Sweden*
[b] *Dipartimento di Chimica G. Ciamician, Università degli Studi di Bologna, via Selmi 2, I-40126 Bologna, Italy*

Received 20 November 2000; accepted 16 December 2000

Abstract

Reaction of $[Os_3(CO)_{11}(NCMe)]$ with R_2S (R = Et, ^{n}Pr) and $MeSBu^t$ results in the formation of $[Os_3(CO)_{11}(L)]$ (L = thioether) clusters in which the thioethers are coordinated in an equatorial site of the triosmium framework. Such monosubstituted clusters are also formed when $[Os_3(CO)_{10}(NCMe)_2]$ is reacted with R_2S (R = Et, ^{n}Pr) while reaction of the same cluster with Ph_2S or MeSPh results in the formation of orthometallated clusters, viz. $[Os_3(\mu\text{-}H)(CO)_{10}(\mu\text{-}\eta^2\text{-}C_6H_4SR)]$ and $[Os_3(\mu\text{-}H)(CO)_9(\mu_3\text{-}C_6H_4SPh)]$. The similar reaction of $[Os_3(\mu\text{-}H)_2(CO)_{10}]$ with Pr_2S, $MeSBu^t$, MeSPh or Ph_2S does not lead to discernable products except when carried out in the presence of trimethylamine N-oxide, which leads to clusters of the general formula $[Os_3(CO)_9(\mu\text{-}H)_2(\text{thioether})]$. The crystal and molecular structures of $[Os_3(CO)_{11}(L)]$ (L = Et_2S, Pr_2S, $S(CH_2)_5$) and $[Os_3(CO)_9(\mu\text{-}H)(\mu\text{-}X)\{SMe(Bu^t)\}]$ (X = H, OH) are presented.

Keywords: Osmium; Cluster; Thioether; Hydrodesulfurization; Crystal structure

1. Introduction

Several models/mechanisms for catalytic hydrodesulfurization (HDS) reactions have been proposed [1]. The initial coordination of the organosulfur substrates to the catalyst surface and the mechanistic details of the catalytic process(es) are not completely understood, although models for the interaction of thiols and thioethers with metal surfaces and subsequent desulfurization reactions have been presented [2]. In order to model possible reaction intermediates in HDS processes, we are currently undertaking a broad study of the interactions of sulfur-containing molecules with transition metal clusters [3–5]. Clusters containing ruthenium, osmium, rhodium and iridium are of special interest since these metals, and especially their sulfides, are known to be good HDS catalysts [1], although the lower cost of molybdenum, and the possibility of promoting the catalytic performance of MoS_2 by the addition of cobalt or nickel, make molybdenum sulfide-based catalysts the choice for industrial HDS catalysis. Our interest in establishing whether the coordination modes of thioethers can be correlated to electronic and/or steric factors, and whether the thioether coordination mode influences the reactivity of the cluster prompted us to study the coordination of thioethers to polynuclear metal complexes.

Previous studies of reactions of thioethers with tetrahedral ruthenium-, cobalt-, and rhodium-containing clusters [6,7] and $[Rh_6(CO)_{16}]$ [8] have demonstrated several bonding modes for thioether ligands. Terminal coordination, bridging ligands in butterfly clusters, and bridging ligands connecting two clusters have been

* Corresponding author. Tel.: +46-46-2228118; fax: +46-46-2224439.
E-mail address: ebbe.nordlander@inorg.lu.se (E. Nordlander).
[1] Present address: Fachhochschule Ansbach, Residenzstr. 8, DE-91522 Ansbach, Germany.

0022-328X/01/$ - see front matter
PII: S0022-328X(01)00643-X

observed. Similarly, Adams and coworkers have shown that thioethers may coordinate to trinuclear clusters in monodentate as well as bridging didentate coordination modes [18,19]. Reactions of alkyl and aryl sulfides with $[M_3(CO)_{12}]$ (M = Ru, Os) afforded the clusters $[Os_3(\mu\text{-}H)(\mu\text{-}SR)(\mu_3\text{-}\eta^2\text{-}C_6H_4)(CO)_9]$ (R = Me, ^{i}Pr) [9] and $[Ru_3(\mu\text{-}SPh)(\mu\text{-}\eta^1;\eta^6\text{-}C_6H_5)(CO)_8]$ [10] as a result of aryl-S cleavage. Furthermore, Adams and coworkers [11,12] have studied the coordination chemistry of strained ring thioethers such as thiirane and thietane with polynuclear metal carbonyl clusters; the release of ring strain in these cyclic thioethers should lead to more facile C–S bond cleavage processes. Thiiranes undergo facile elimination of sulfur to yield the corresponding olefin. Metal atoms promote the desulfurization, and through this reaction these molecules have been found to serve as clean sources of monoatomic sulfur for use in the synthesis of polynuclear metal complexes containing sulfido ligands. Unlike thiiranes, thietanes can serve as effective ligands in metal complexes through the coordination of one or both of the lone pairs of electrons on the sulfur atom, which has resulted in

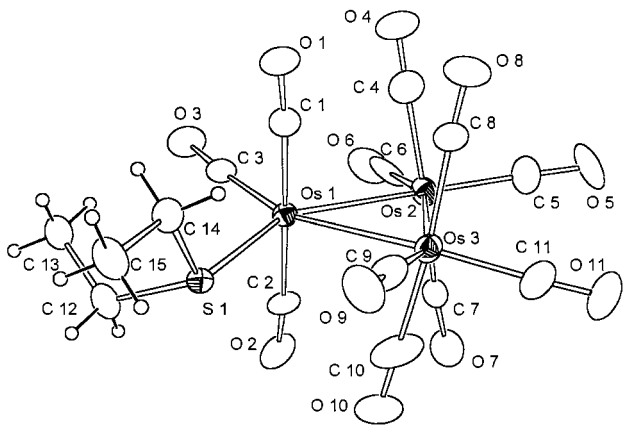

Fig. 1. An ORTEP plot of the molecular structure of $[Os_3(CO)_{11}(SEt_2)]$ **1**, showing the atom labelling scheme. Thermal ellipsoids are drawn at the 30% probability level.

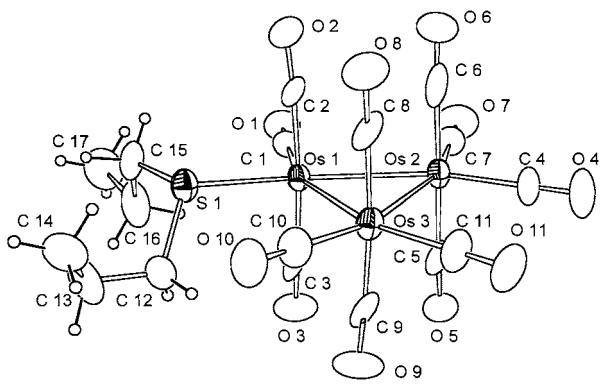

Fig. 2. An ORTEP plot of the molecular structure of $[Os_3(CO)_{11}(SPr_2)]$ **2**, showing the atom labelling scheme. Thermal ellipsoids are drawn at the 30% probability level.

complexes containing both terminally coordinated and bridging ligands between two metal atoms [13–16]. UV–vis irradiation/photolysis of $[Os_3(CO)_{11}\{S(CH_2)_3\}]$ [17] or the dimethyl homologue $[Os_3(CO)_{11}(SCH_2CMe_2CH_2)]$ [14] has been shown to lead to ring-opening and formation of clusters containing thiametallacyclic rings. A facile ring-opening transformation of tetrahydrothiophene by a triosmium cluster complex has also been reported [18]; both C–H and C–S cleavage were observed.

Here, we wish to report the reactions of a number of thioethers with $[Os_3(CO)_{12-n}(NCMe)_n]$ ($n = 1,2$) and $[Os_3(\mu\text{-}H)_2(CO)_{10}]$, which have led to the isolation of several new clusters of general formulae $[Os_3(CO)_{11}(L)]$ and $[Os_3(\mu\text{-}H)_2(CO)_9(L)]$ (L = thioether). When aryl sulfides were used as ligands, triosmium clusters containing orthometallated phenyl substituents could be isolated.

2. Results and discussion

2.1. Reaction of $[Os_3(CO)_{11}(NCMe)]$ with R_2S (R = Et, ^{n}Pr) and MeSBu^t

In order to prepare clusters with thioethers in monodentate coordination modes, 1–1.5 equivalents of an appropriate thioether ligand L was added to a dichloromethane solution of $[Os_3(CO)_{11}(NCMe)]$ at room temperature, leading to the formation of $[Os_3(CO)_{11}(L)]$ [L = Et_2S (**1**), Pr_2S (**2**), MeSBu^t (**3**)] in moderate to good yields (20–60%). In addition, the previously reported cluster $[Os_3(CO)_{11}\{S(CH_2)_5\}]$ (**4**) [19], containing the cyclic pentamethylene sulfide ligand, was isolated in low yield from the reaction of the ligand with $[Os_3(CO)_{10}(NCMe)_2]$ (vide infra). The products were identified by IR and ^{1}H-NMR spectroscopy as well as mass spectrometry. Comparison of the ν_{C-O} IR stretching patterns of **1**–**4** to those of known clusters [19] indicated that the thioethers were in all cases coordinated in equatorial positions on the trinuclear cluster framework.

2.2. Crystal and molecular structures of $[Os_3(CO)_{11}(L)]$ [L = Et_2S (**1**), Pr_2S (**2**), $S(CH_2)_5$ (**4**)]

It was possible to grow yellow crystals of **1**, **2**, and **4** by slow evaporation of dichloromethane–hexane solutions at 4°C; in order to confirm the equatorial coordination of the thioethers in these clusters, their molecular structures were determined by X-ray diffraction. The molecular structures of compounds **1**, **2** and **4** are illustrated in Figs. 1–3 and selected bond lengths and angles are listed in Tables 1–3. In each compound, the osmium atoms form an irregular triangle with all three Os–Os distances being inequivalent, and the

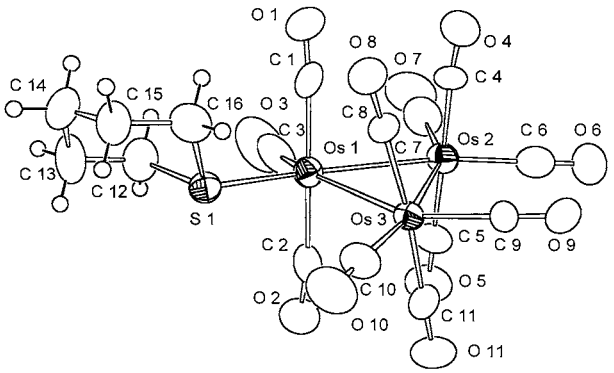

Fig. 3. An ORTEP plot of the molecular structure of $[Os_3(CO)_{11}\{S(CH_2)_5\}]$ **5**, showing the atom labelling scheme. Thermal ellipsoids are drawn at the 30% probability level.

Table 1
Selected bond lengths (Å) and angles (°) for $[Os_3(CO)_{11}(SEt_2)]$ (**1**)

Bond lengths			
Os(1)–Os(2)	2.841(1)	Os(2)–C(5)	1.89(2)
Os(1)–Os(3)	2.886(1)	C(5)–O(5)	1.18(2)
Os(2)–Os(3)	2.876(2)	Os(2)–C(6)	1.89(2)
Os(1)–S(1)	2.400(4)	C(6)–O(6)	1.14(2)
S(1)–C(12)	1.84(2)	Os(2)–C(7)	1.96(2)
S(1)–C(14)	1.79(2)	C(7)–O(7)	1.12(2)
Os(1)–C(1)	1.91(2)	Os(3)–C(8)	1.95(2)
C(1)–O(1)	1.15(2)	C(8)–O(8)	1.14(2)
Os(1)–C(2)	1.94(2)	Os(3)–C(9)	1.90(2)
C(2)–O(2)	1.14(2)	C(9)–O(9)	1.17(3)
Os(1)–C(3)	1.88(2)	Os(3)–C(10)	1.94(3)
C(3)–O(3)	1.14(2)	C(10)–O(10)	1.11(3)
Os(2)–C(4)	1.98(2)	Os(3)–C(11)	1.89(3)
C(4)–O(4)	1.13(3)	C(11)–O(11)	1.14(3)
Bond angles			
Os(2)–Os(1)–Os(3)	60.28(3)	C(5)–Os(2)–Os(1)	154.9(7)
C(1)–Os(1)–C(2)	179.1(9)	C(5)–Os(2)–Os(3)	95.8(7)
C(1)–Os(1)–C(3)	90.7(8)	C(6)–Os(2)–Os(1)	99.0(7)
C(2)–Os(1)–C(3)	88.7(8)	C(6)–Os(2)–Os(3)	158.6(6)
S(1)–Os(1)–C(1)	91.0(6)	C(7)–Os(2)–Os(1)	93.5(6)
S(1)–Os(1)–C(2)	88.5(6)	C(7)–Os(2)–Os(3)	84.2(7)
S(1)–Os(1)–C(3)	105.7(6)	Os(1)–Os(3)–Os(2)	59.09(3)
S(1)–Os(1)–Os(2)	151.52(9)	C(8)–Os(3)–C(9)	94.2(9)
S(1)–Os(1)–Os(3)	93.6(1)	C(8)–Os(3)–C(10)	173.1(9)
C(1)–Os(1)–Os(2)	96.1(6)	C(8)–Os(3)–C(11)	94(1)
C(1)–Os(1)–Os(3)	82.7(6)	C(9)–Os(3)–C(10)	89(1)
C(2)–Os(1)–Os(2)	84.7(6)	C(9)–Os(3)–C(11)	102(1)
C(2)–Os(1)–Os(3)	98.0(6)	C(10)–Os(3)–C(11)	92(1)
C(3)–Os(1)–Os(2)	101.8(5)	C(8)–Os(3)–Os(1)	94.1(6)
C(3)–Os(1)–Os(3)	159.8(6)	C(8)–Os(3)–Os(2)	81.6(5)
Os(1)–Os(2)–Os(3)	60.62(3)	C(9)–Os(3)–Os(1)	99.2(6)
C(4)–Os(2)–C(5)	91(1)	C(9)–Os(3)–Os(2)	157.2(6)
C(4)–Os(2)–C(6)	88.3(9)	C(10)–Os(3)–Os(1)	79.2(8)
C(4)–Os(2)–C(7)	176.8(9)	C(10)–Os(3)–Os(2)	93.3(7)
C(5)–Os(2)–C(6)	105.2(9)	C(11)–Os(3)–Os(1)	156.7(8)
C(5)–Os(2)–C(7)	92(1)	C(11)–Os(3)–Os(2)	100.6(9)
C(6)–Os(2)–C(7)	91(1)	C(12)–S(1)–C(14)	102(1)
C(4)–Os(2)–Os(1)	83.5(6)	C(12)–S(1)–Os(1)	111.0(6)
C(4)–Os(2)–Os(3)	95.2(5)	C(14)–S(1)–Os(1)	111.4(6)

thioether ligand is coordinated via the sulfur atom at an equatorial coordination site of one Os atom. The average Os–Os distances [2.868 Å (**1**), 2.860 Å (**2**), 2.872 Å (**4**)] are slightly shorter than those found in the parent compound, $[Os_3(CO)_{12}]$ [$Os–Os_{ave} = 2.877(3)$ Å] [20]. A general trend in metal–metal distances is observed; the longest Os–Os interactions in **1**, **2** and **4** [Os(1)–Os(3) 2.886(1), 2.881(2) and 2.894(1) Å, respectively] are in *cis* position with respect to the S atom of the thioether ligand, presumably in order to alleviate steric crowding. On the other hand, the shortest Os–Os separations [Os(1)–Os(2) = 2.841(1), 2.822(2) and 2.847(1) Å, respectively] are those *trans* to the S atoms as the presence of good σ donors causes a contraction of the M–M bond in *trans* position [21]. The Os–S distances for **1**, **2** and **4** [2.400(4), 2.398(3) and 2.406(4) Å, respectively] are similar to those found in the terminally coordinated compounds $[Os_3(CO)_{11}\{S(CH_2)_3\}]$ [17], $[Os_3(CO)_{10}\{S(CH_2)_4\}_2]$ [18] and in the complex $[Os_3(CO)_8(\mu\text{-}SCH_2CH_2CH_2CH_2C)\{S(CH_2)_5\}(\mu\text{-}H)_2]$ [19] which contains one terminally coordinated pentamethylene sulfide ligand and one bridging an Os–Os bond [Os–S = 2.375(5), 2.404(ave) and 2.396(3) (terminal) Å, respectively]. The pentamethylene sulfide ligand in compound **4** adopts the stable chair conformation as was also found for the terminal thioether in $[Os_3(CO)_8(\mu\text{-}SCH_2CH_2CH_2CH_2C)(S(CH_2)_5)(\mu\text{-}H)_2]$ [19]. It is worth noting that in **1** and **4** there is significant tilting of the $Os(CO)_4$ and of the $Os(CO)_3(SR_2)$ groups with respect to the Os_3 plane. This distortion occurs presumably to reduce the steric interaction between the thioether ligand and the axial carbonyls that face the same side of the molecule.

2.3. Reaction of $[Os_3(CO)_{10}(NCMe)_2]$ with Et_2S, Pr_2S, $S(CH_2)_5$, MeSPh and SPh_2

It is well established that the reaction of $[Os_3(CO)_{10}(NCMe)_2]$ with two-electron donors in general leads to the formation of disubstituted complexes [22], but the reaction of $[Os_3(CO)_{10}(NCMe)_2]$ with 3,3-dimethylthietane is an exception which yields only the *mono*-thietane complex $[Os_3(CO)_{10}(\mu\text{-}SCH_2CMe_2CH_2)]$, in which the ligand is bridging two osmium atoms through the sulfur [14]. With the aim of preparing similar clusters with didentate bridging thioethers, $[Os_3(CO)_{10}(NCMe)_2]$ was reacted with Et_2S, Pr_2S, $S(CH_2)_5$, and Ph_2S; however, in no case could the desired product, $[Os_3(CO)_{10}(\mu\text{-}SR_2)]$, be obtained. Somewhat surprisingly, the only products that could be isolated from the reactions of $[Os_3(CO)_{10}(NCMe)_2]$ with Et_2S or Pr_2S were the monosubstituted clusters **1** and **2** (vide supra) which were identified by IR spectroscopy and mass spectrometry. These products must be due to (relatively complex) disproportionation reactions. Presumably, these reactions occur via initial formation of

$[Os_3(CO)_{10}(NCMe)(SR_2)]$ and subsequent abstraction of a CO ligand from a second cluster to form the product. The adventitious presence of $[Os_3(CO)_{11}(NCMe)]$ may also be the cause of formation of some product, but the relatively high yields of the reactions (50–60%) may not be ascribed to the presence of the *mono*-acetonitrile cluster (assuming that any amount of carbon monoxide may be abstracted from a single cluster, the theoretical yield for a CO disproportionation reaction would be 90%).

As has been previously observed by Adams and coworkers [19], reaction of the cyclic thioether pentamethylene sulfide, $S(CH_2)_5$, with $[Os_3(CO)_{10}(NCMe)_2]$ resulted in the formation of a bright yellow product which could be identified as the disubstituted cluster $[Os_3(CO)_{10}\{S(CH_2)_5\}_2]$ **5** on the basis of IR spectroscopy and mass spectrometry (cf. [19]). A small amount of $[Os_3(CO)_{11}\{S(CH_2)_5\}]$ (**4**) (vide supra) was also formed. To our knowledge, **5** and the corresponding tetrahydrothiophene cluster $[Os_3(CO)_{10}(SC_4H_8)_2]$ [18] are the only examples of multiple thioether substitution on a triosmium cluster. The reasons for the relative stabilities of $[Os_3(CO)_{10}(\mu\text{-}SR_2)]$ vs. $[Os_3(CO)_{10}(SR_2)_2]$ are unclear. In either case, an initial intermediate, '$[Os_3(CO)_{10}(SR_2)(NCMe)]$', may be envisaged, and the capability of the thioether to act as a four-electron bridging ligand is likely to determine which product is formed (Scheme 1). It may thus be expected that thioethers with good σ-donor capabilities (e.g. SMe_2) will be prone to coordinate in briding modes.

Table 2
Selected bond lengths (Å) and angles (°) for $[Os_3(CO)_{11}(SPr_2)]$ (**2**)

Bond lengths			
Os(1)–Os(2)	2.822(2)	Os(2)–C(5)	1.91(1)
Os(1)–Os(3)	2.881(2)	C(5)–O(5)	1.16(1)
Os(2)–Os(3)	2.877(1)	Os(2)–C(6)	1.89(2)
Os(1)–S(1)	2.406(4)	C(6)–O(6)	1.19(2)
S(1)–C(12)	1.81(1)	Os(2)–C(7)	1.89(1)
S(1)–C(15)	1.83(2)	C(7)–O(7)	1.13(1)
Os(1)–C(1)	1.88(1)	Os(3)–C(8)	1.91(1)
C(1)–O(1)	1.13(1)	C(8)–O(8)	1.17(1)
Os(1)–C(2)	1.89(1)	Os(3)–C(9)	1.91(1)
C(2)–O(2)	1.22(1)	C(9)–O(9)	1.16(1)
Os(1)–C(3)	1.87(1)	Os(3)–C(10)	1.89(1)
C(3)–O(3)	1.17(1)	C(10)–O(10)	1.13(2)
Os(2)–C(4)	1.90(1)	Os(3)–C(11)	1.90(1)
C(4)–O(4)	1.11(1)	C(11)–O(11)	1.13(2)
Bond angles			
Os(2)–Os(1)–Os(3)	60.59(5)	C(5)–Os(2)–Os(1)	88.4(4)
C(1)–Os(1)–C(2)	89.7(5)	C(5)–Os(2)–Os(3)	89.7(3)
C(1)–Os(1)–C(3)	89.7(5)	C(6)–Os(2)–Os(1)	90.1(4)
C(2)–Os(1)–C(3)	175.3(5)	C(6)–Os(2)–Os(3)	90.6(4)
S(1)–Os(1)–C(1)	102.9(4)	C(7)–Os(2)–Os(1)	100.2(5)
S(1)–Os(1)–C(2)	83.2(3)	C(7)–Os(2)–Os(3)	160.9(5)
S(1)–Os(1)–C(3)	92.4(2)	Os(1)–Os(3)–Os(2)	58.69(5)
S(1)–Os(1)–Os(2)	157.05(9)	C(8)–Os(3)–C(9)	174.2(6)
S(1)–Os(1)–Os(3)	97.2(1)	C(8)–Os(3)–C(10)	87.9(7)
C(1)–Os(1)–Os(2)	99.0(4)	C(8)–Os(3)–C(11)	93.9(7)
C(1)–Os(1)–Os(3)	159.5(4)	C(9)–Os(3)–C(10)	91.4(6)
C(2)–Os(1)–Os(2)	90.3(3)	C(9)–Os(3)–C(11)	91.8(8)
C(2)–Os(1)–Os(3)	89.1(3)	C(10)–Os(3)–C(11)	102.4(7)
C(3)–Os(1)–Os(2)	94.4(4)	C(8)–Os(3)–Os(1)	89.8(4)
C(3)–Os(1)–Os(3)	93.1(4)	C(8)–Os(3)–Os(2)	88.8(4)
Os(1)–Os(2)–Os(3)	60.72(5)	C(9)–Os(3)–Os(1)	84.8(4)
C(4)–Os(2)–C(5)	90.6(7)	C(9)–Os(3)–Os(2)	90.1(3)
C(4)–Os(2)–C(6)	91.3(7)	C(10)–Os(3)–Os(1)	103.9(4)
C(4)–Os(2)–C(7)	103.4(7)	C(10)–Os(3)–Os(2)	162.3(4)
C(5)–Os(2)–C(6)	178.0(6)	C(11)–Os(3)–Os(1)	153.6(6)
C(5)–Os(2)–C(7)	90.0(6)	C(11)–Os(3)–Os(2)	95.3(6)
C(6)–Os(2)–C(7)	89.1(6)	C(12)–S(1)–C(15)	103.7(8)
C(4)–Os(2)–Os(1)	156.4(5)	C(12)–S(1)–Os(1)	110.9(6)
C(4)–Os(2)–Os(3)	95.7(5)	C(15)–S(1)–Os(1)	108.5(5)

Table 3
Selected bond lengths (Å) and angles (°) for $[Os_3(CO)_{11}\{S(CH_2)_5\}]$ (**4**)

Bond lengths			
Os(1)–Os(2)	2.847(1)	Os(2)–C(5)	1.92(1)
Os(1)–Os(3)	2.894(1)	C(5)–O(5)	1.15(2)
Os(2)–Os(3)	2.876(1)	Os(2)–C(6)	1.91(2)
Os(1)–S(1)	2.398(3)	C(6)–O(6)	1.13(2)
S(1)–C(12)	1.80(1)	Os(2)–C(7)	1.88(2)
S(1)–C(16)	1.80(1)	C(7)–O(7)	1.16(2)
Os(1)–C(1)	1.92(1)	Os(3)–C(8)	1.90(1)
C(1)–O(1)	1.14(1)	C(8)–O(8)	1.14(1)
Os(1)–C(2)	1.94(2)	Os(3)–C(9)	1.90(1)
C(2)–O(2)	1.14(2)	C(9)–O(9)	1.14(1)
Os(1)–C(3)	1.83(2)	Os(3)–C(10)	1.89(1)
C(3)–O(3)	1.16(2)	C(10)–O(10)	1.15(2)
Os(2)–C(4)	1.92(1)	Os(3)–C(11)	1.94(1)
C(4)–O(4)	1.14(1)	C(11)–O(11)	1.14(1)
Bond angles			
Os(2)–Os(1)–Os(3)	60.14(3)	C(5)–Os(2)–Os(1)	85.4(4)
C(1)–Os(1)–C(2)	178.2(5)	C(5)–Os(2)–Os(3)	90.9(4)
C(1)–Os(1)–C(3)	89.3(6)	C(6)–Os(2)–Os(1)	165.6(4)
C(2)–Os(1)–C(3)	92.5(6)	C(6)–Os(2)–Os(3)	105.1(4)
S(1)–Os(1)–C(1)	91.7(4)	C(7)–Os(2)–Os(1)	93.0(5)
S(1)–Os(1)–C(2)	87.5(4)	C(7)–Os(2)–Os(3)	153.2(5)
S(1)–Os(1)–C(3)	100.7(5)	Os(1)–Os(3)–Os(2)	59.12(3)
S(1)–Os(1)–Os(2)	159.47(8)	C(8)–Os(3)–C(9)	95.4(5)
S(1)–Os(1)–Os(3)	100.23(9)	C(8)–Os(3)–C(10)	88.7(5)
C(1)–Os(1)–Os(2)	85.6(4)	C(8)–Os(3)–C(11)	174.3(5)
C(1)–Os(1)–Os(3)	97.8(4)	C(9)–Os(3)–C(10)	100.9(6)
C(2)–Os(1)–Os(2)	94.5(4)	C(9)–Os(3)–C(11)	90.3(5)
C(2)–Os(1)–Os(3)	80.7(4)	C(10)–Os(3)–C(11)	89.9(5)
C(3)–Os(1)–Os(2)	99.6(5)	C(8)–Os(3)–Os(1)	79.1(3)
C(3)–Os(1)–Os(3)	157.6(5)	C(8)–Os(3)–Os(2)	92.4(3)
Os(1)–Os(2)–Os(3)	60.74(3)	C(9)–Os(3)–Os(1)	152.1(4)
C(4)–Os(2)–C(5)	174.5(5)	C(9)–Os(3)–Os(2)	94.2(4)
C(4)–Os(2)–C(6)	88.5(6)	C(10)–Os(3)–Os(1)	106.2(4)
C(4)–Os(2)–C(7)	92.6(6)	C(10)–Os(3)–Os(2)	164.7(4)
C(5)–Os(2)–C(6)	92.7(6)	C(11)–Os(3)–Os(1)	96.0(3)
C(5)–Os(2)–C(7)	92.3(6)	C(11)–Os(3)–Os(2)	87.5(4)
C(6)–Os(2)–C(7)	101.4(6)	C(12)–S(1)–C(16)	97.3(7)
C(4)–Os(2)–Os(1)	92.1(3)	C(12)–S(1)–Os(1)	107.1(5)
C(4)–Os(2)–Os(3)	83.6(3)	C(16)–S(1)–Os(1)	111.8(4)

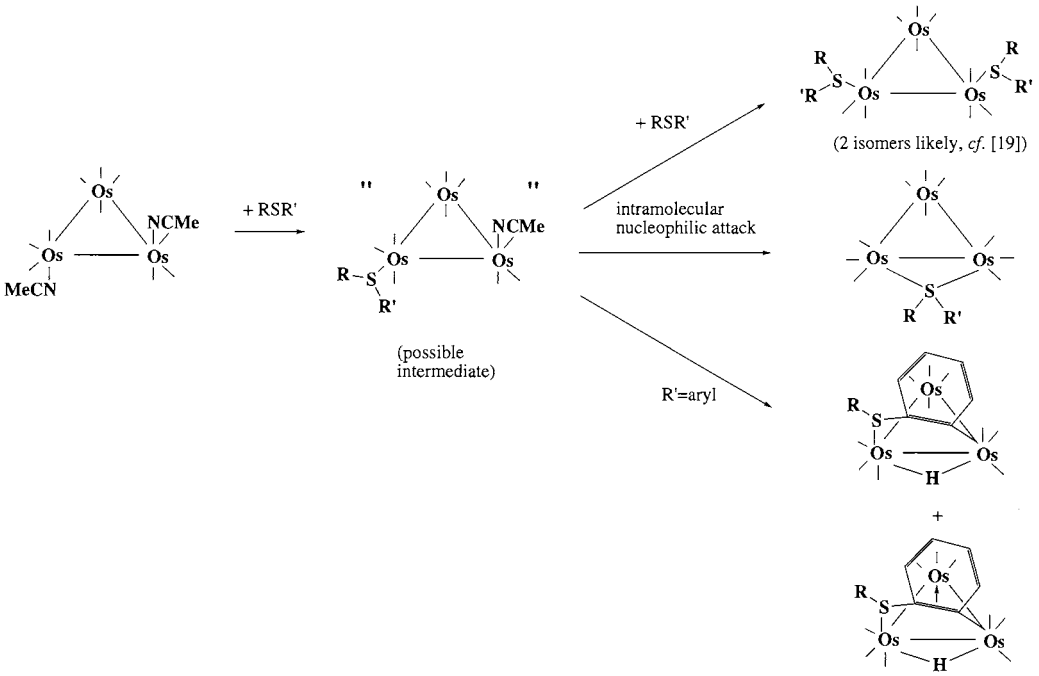

Scheme 1. Schematic depiction of reactions of $[Os_3(CO)_{10}(NCMe)_2]$ with thioethers observed in this work and by Adams and coworkers [14,18,19]. Formation of mono-substituted $[Os_3(CO)_{11}(thioether)]$ has also been observed, see text.

Reaction of $[Os_3(CO)_{10}(NCMe)_2]$ with the phenyl containing ligands SPh_2 or MeSPh, under the same conditions as above, resulted in C–H activation and metallation of the phenyl substituent rather than thioether coordination on the trinuclear cluster. In the case of Ph_2S, two products were isolated and identified. The ^{1}H-NMR of the first, major, product showed a resonance at -14.41 ppm, consistent with the presence of a bridging hydride, and three signals assigned to a cyclometallated μ-C_6H_4 moiety were observed at 8.04 (d, 1H), 6.92 (m, 2H) and 6.74 (t, 1H) ppm. The IR pattern of this product is very similar to the known $[Os_3(CO)_{10}\{\mu$-$PhSC_2CH_2C(Me)Bu^t\}(\mu$-$H)]$ [23] and the product is therefore proposed to be $[Os_3(\mu$-$H)(CO)_{10}(\mu$-η^2-$C_6H_4SPh)]$ (**6**); the mass spectrum of **6** is fully consistent with this formulation. The second product was isolated in low yield and identified as $[Os_3(\mu$-$H)(CO)_9(\mu_3$-$C_6H_4SPh)]$ (**7**) on the basis of ^{1}H-NMR, IR and mass spectrometry. A hydride signal at -14.85 ppm and resonances at 5.85 (d, 1H), 6.70 (t, 1H), 6.92 (t, 1H) and 7.89 (d, 1H) in the ^{1}H-NMR spectrum of **7** are consistent with an ortho-metallated phenyl moiety. The ν_{C-O} IR stretching pattern is similar to that of the known $[Os_3(CO)_9\{\mu_3$-$PhSC_2CH_2C(Me)Bu^t\}(\mu$-$H)]$ [23] and the mass spectrum is consistent with the above-mentioned formulation. Similarly, $[Os_3(\mu$-$H)(CO)_{10}(\mu$-η^2-$SC_6H_4Me)]$ was the major product observed in the reaction with MeSPh. The ν_{C-O} IR stretching pattern is identical to that of compound **6** and a hydride peak is observed in the ^{1}H-NMR at -14.7 ppm. The reactions of $[Os_3(CO)_{10}(NCMe)_2]$ with thioethers may be summarized by Scheme 1.

2.4. Treatment of $[Os_3(\mu$-$H)_2(CO)_{10}]$ with Pr_2S, $MeSBu^t$ or Ph_2S in the presence of Me_3NO

It has been shown that reactions between $[Os_3(\mu$-$H)_2(CO)_{10}]$ and tertiary phosphines lead to clusters of the type $[HOs_3(\mu$-$H)(CO)_{10}(L)]$, which can exist in several different structural isomers in which the phosphine is known to coordinate in both axial and equatorial sites on the trinuclear cluster [24,25]. The sum of the Taft σ^* constants for the substituents of thioethers have been used as estimates of the relative σ-donor strengths of thioethers [26]; in addition, cone angles (θ) for a number of thioethers have been derived [26,27] and combinations of the two factors have been used to describe the relative nucleophilicity of thioethers [26,27]. Although the variations in cone angles and σ-donor strengths for the thioethers used in this study are relatively small[2], it is nevertheless possible that these properties may give rise to different coordination modes in putative $[HOs_3(\mu$-$H)(CO)_{10}(RSR')]$ clusters. In an attempt to obtain $[HOs_3(\mu$-$H)(CO)_{10}(L)]$ clusters (L = thioether) and ascertain the coordination modes of the sulfur ligands in such clusters, $[Os_3(\mu$-$H)_2(CO)_{10}]$ was reacted with one equivalent of SPh_2 or $MeSBu^t$ in dichloromethane at ambient temperature. No reaction

[2] For the thioethers studied here, the values are Et_2S: $\theta = 88°$, $\sigma^* = -0.20$; Pr_2S: $\theta = 88°$, $\sigma^* = -0.23$; $MeSBu^t$: $\theta = 100°$, $\sigma^* = -0.30$ (average of values for Me_2S and $^tBu_2S$); $S(CH_2)_5$: $\theta = 82°$ (based on the cone angle for 1,4-thioxane, derived from experimental data [26]); Ph_2S: $\theta = 97°$, MeSPh: $\theta = 88°$ (data taken from [26,27])

could be observed after 20 h in either case, and reflux of the reaction mixtures at 40°C for another 4 h resulted in decomposition.

However, treatment of $[Os_3(\mu\text{-}H)_2(CO)_{10}]$ with equimolar amounts of Me_3NO and an appropriate thioether (Pr_2S, $MeSBu^t$, Ph_2S) resulted in a change of color from purple to red and the formation of new clusters of the general formula $[Os_3(\mu\text{-}H)_2(CO)_9(L)]$ [L = Pr_2S (**8**), Ph_2S (**9**), $MeSBu^t$ (**10**)]. Addition of trimethylamine N-oxide to carbonyl complexes generates coordinative unsaturation via the oxidation of CO to CO_2; the coordinative unsaturation may be (lightly) stabilized by coordination of NMe_3. A possible coordinatively unsaturated species formed from $[Os_3(\mu\text{-}H)_2(CO)_{10}]$ would be '$[Os_3(\mu\text{-}H)_2(CO)_9]$' which may be expected to be very electrophilic as it would be a four-electron deficient 44e$^-$ cluster; this explains the ready addition of thioethers which appear to be relatively poor nucleophiles. While the hydrides in $[Os_3(\mu\text{-}H)_2(CO)_{10}]$ and $[HOs_3(\mu\text{-}H)(CO)_{10}(L)]$ (L = phosphine) [24,25] are fluxional at ambient temperature, the bridging hydrides in **8**–**10** give rise to a signal at approximately -10 ppm in the ^{1}H-NMR spectrum for each cluster. The IR spectra of **8**–**10** show similar ν(CO) resonances as known compounds of the type $[Os_3(\mu\text{-}H)_2(CO)_9(L)]$ (L = PMe_2Ph, PPh_3) [28], and in the case of **9**, the molecular structure has been determined by an X-ray diffraction study. In the reaction with $MeSBu^t$, a minor product was isolated and characterized as $[Os_3(CO)_9(\mu\text{-}H)(\mu\text{-}OH)\{SMe(Bu^t)\}]$ **11** by X-ray crystallography. The formation of **11** is very likely due to the adventitious presence of water in the solvent(s) used in the reaction and/or workup of the crude reaction product.

2.5. Crystal and molecular structures of $[Os_3(CO)_9(\mu\text{-}H)_2\{SMe(Bu^t)\}]$ **10** and $[Os_3(CO)_9(\mu\text{-}H)(\mu\text{-}OH)\{SMe(Bu^t)\}]$ **11**

Dark red crystals of $[Os_3(CO)_9(\mu\text{-}H)_2\{SMe(Bu^t)\}]$ **10** were grown by slow evaporation of a dichloromethane-hexane solution at 4°C. The molecular structure of **10** is illustrated in Fig. 4 and selected bond lengths and angles are listed in Table 4. The molecule consists of a triangle of osmium atoms where one osmium atom coordinates to four terminal carbonyls and the remaining two osmium atoms [Os(1) and Os(2)] coordinate to two and three terminal carbonyls, respectively. The Os(1)–Os(2) bond is doubly bridged by two hydrides; in addition, $MeSBu^t$ is terminally coordinated to Os(1) in an equatorial coordination site. The Os(1)–Os(2) distance [2.683(1) Å] is almost identical to that found in the parent $[Os_3(\mu\text{-}H)_2(CO)_{10}]$ [2.681(1) Å] [29] and the phosphine-substituted $[Os_3(\mu\text{-}H)_2(CO)_9(PPh_3)]$

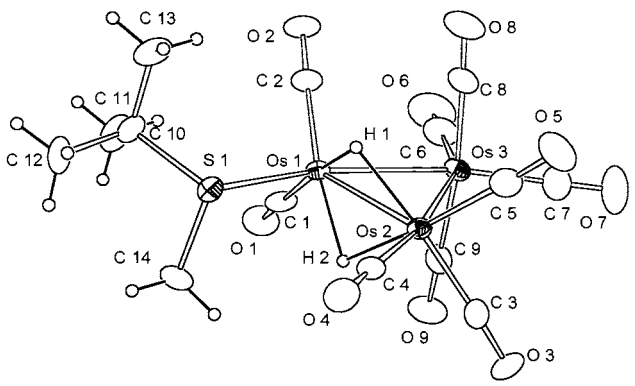

Fig. 4. An ORTEP plot of the molecular structure of $[Os_3(CO)_9(\mu\text{-}H)_2(SMe^tBu)]$ **10**, showing the atom labelling scheme. Thermal ellipsoids are drawn at the 30% probability level.

Table 4
Selected bond lengths (Å) and angles (°) for $[Os_3(CO)_9(\mu\text{-}H)_2\{SMe(Bu^t)\}]$ (**10**)

Bond lengths			
Os(1)–Os(2)	2.683(1)	Os(2)–C(4)	1.92(1)
Os(1)–Os(3)	2.785(1)	C(4)–O(4)	1.11(1)
Os(2)–Os(3)	2.797(1)	Os(2)–C(5)	1.92(1)
S(1)–Os(1)	2.418(3)	C(5)–O(5)	1.12(1)
S(1)–C(10)	1.85(1)	Os(3)–C(6)	1.90(1)
S(1)–C(14)	1.81(1)	C(6)–O(6)	1.13(1)
Os(1)–C(1)	1.86(1)	Os(3)–C(7)	1.91(1)
C(1)–O(1)	1.14(1)	C(7)–O(7)	1.13(2)
Os(1)–C(2)	1.86(1)	Os(3)–C(8)	1.94(1)
C(2)–O(2)	1.13(1)	C(8)–O(8)	1.14(1)
Os(2)–C(3)	1.89(1)	Os(3)–C(9)	1.94(1)
C(3)–O(3)	1.15(1)	C(9)–O(9)	1.13(1)
Bond angles			
Os(2)–Os(1)–Os(3)	61.49(3)	C(5)–Os(2)–H(2)	172(3)
C(1)–Os(1)–C(2)	88.8(5)	C(3)–Os(2)–Os(1)	127.5(3)
C(1)–Os(1)–H(1)	174(3)	C(3)–Os(2)–Os(3)	91.7(3)
C(1)–Os(1)–H(2)	94(2)	C(4)–Os(2)–Os(1)	108.2(3)
C(1)–Os(1)–S(1)	97.8(4)	C(4)–Os(2)–Os(3)	169.3(3)
C(2)–Os(1)–H(1)	98(2)	C(5)–Os(2)–Os(1)	130.1(3)
C(2)–Os(1)–H(2)	172(3)	C(5)–Os(2)–Os(3)	91.0(3)
C(2)–Os(1)–S(1)	104.2(4)	H(1)–Os(2)–Os(1)	43.5(6)
S(1)–Os(1)–H(1)	79(4)	H(1)–Os(2)–Os(3)	83(3)
S(1)–Os(1)–H(2)	83(4)	H(2)–Os(2)–Os(1)	43.5(6)
S(1)–Os(1)–Os(2)	97.22(7)	H(2)–Os(2)–Os(3)	82(3)
S(1)–Os(1)–Os(3)	158.66(6)	Os(1)–Os(3)–Os(2)	57.46(3)
C(1)–Os(1)–Os(2)	131.9(3)	C(6)–Os(3)–C(7)	101.2(6)
C(1)–Os(1)–Os(3)	98.2(4)	C(6)–Os(3)–C(8)	95.5(5)
C(2)–Os(1)–Os(2)	130.5(4)	C(6)–Os(3)–C(9)	91.2(5)
C(2)–Os(1)–Os(3)	90.2(4)	C(7)–Os(3)–C(8)	94.2(6)
H(1)–Os(1)–Os(2)	43.8(6)	C(7)–Os(3)–C(9)	93.0(5)
H(1)–Os(1)–Os(3)	84(3)	C(8)–Os(3)–C(9)	169.0(5)
H(2)–Os(1)–Os(2)	43.6(6)	C(6)–Os(3)–Os(1)	98.7(5)
H(2)–Os(1)–Os(3)	82(3)	C(6)–Os(3)–Os(2)	156.1(5)
Os(1)–Os(2)–Os(3)	61.05(3)	C(7)–Os(3)–Os(1)	160.1(4)
C(3)–Os(2)–C(4)	95.6(4)	C(7)–Os(3)–Os(2)	102.6(4)
C(3)–Os(2)–C(5)	90.5(5)	C(8)–Os(3)–Os(1)	84.1(4)
C(3)–Os(2)–H(1)	171.0(7)	C(8)–Os(3)–Os(2)	84.9(3)
C(3)–Os(2)–H(2)	92(2)	C(9)–Os(3)–Os(1)	86.3(3)
C(4)–Os(2)–C(5)	96.8(4)	C(9)–Os(3)–Os(2)	85.4(3)
C(4)–Os(2)–H(1)	89(4)	C(10)–S(1)–C(14)	102.7(6)
C(4)–Os(2)–H(2)	90(4)	C(10)–S(1)–Os(1)	115.8(4)
C(5)–Os(2)–H(1)	97(2)	C(14)–S(1)–Os(1)	105.9(4)

[2.683(2)Å] [30] and is very close to that found in $[Os_3(\mu\text{-}H)_2(CO)_9(phosphine)]$ (phosphine = PMe_2Ph [28], P^iPr_3 [31], P^tBu_3 [32]) where the corresponding distances are 2.703(1), 2.689(1) and 2.690(1) Å, respectively. This demonstrates that the $Os(\mu\text{-}H)_2Os$ unit is very little perturbed on ligand substitution. The other two Os–Os bonds are slightly shorter [2.785(1) and 2.797(1) Å] than those found in $[Os_3(\mu\text{-}H)_2(CO)_9(P^iPr_3)]$ [2.816(1) and 2.822(1) Å] [31] and $[Os_3(\mu\text{-}H)_2(CO)_{10}]$ [2.815 and 2.814 Å] [29] and the Os–Os bond *trans* to S is the shortest, as was also found for **1**, **2** and **4** (vide supra). The Os–S bond length [2.418(3) Å] is slightly longer than the analogous Os–S distances [range 2.38–2.40 Å] found in the terminally coordinated triosmium cluster complexes discussed above.

Orange crystals of $[Os_3(CO)_9(\mu\text{-}H)(\mu\text{-}OH)\{SMe(Bu^t)\}]$ **11** were grown by slow evaporation of a dichloromethane solution at room temperature. The molecular structure of **11** is shown in Fig. 5 and selected bond lengths and angles are listed in Table 5. Compound **11** differs from $[Os_3(CO)_9(\mu\text{-}H)_2\{SMe(Bu^t)\}]$ **10** by the presence of a bridging OH group which replaces one of the two bridging hydrides. As a result of this substitution, the unsaturated $46e^-$ cluster **10** becomes the saturated $48e^-$ cluster **11**; thus, a direct comparison of the 46 and 48 electron species can be undertaken. In addition to the S atom of the thioether, the oxygen of the bridging hydroxy ligand is a chiral center as it is coordinated to two non-equivalent Os atoms and *exo* or *endo* configurations (referring to the relative position of the hydrogen of the OH moiety to the osmium triangle [33]) are possible. The μ-OH moiety spans the Os(1)–Os(2) bond symmetrically [Os–O 2.146(7) and 2.142(7) Å]. The doubly bridged Os(1)–Os(2) bond distance of 2.809(1) Å is the shortest of the three metal–metal bonds and strictly comparable to that found in $[Os_3(CO)_9(\mu\text{-}H)(\mu\text{-}OH)]$ [2.806(1) Å] [34]. This can be attributed to the shortening effect of the bridging hydroxy group prevailing on the lengthening effect of the bridging hydride. The two remaining Os–Os bonds are longer than the analogous distances in **10** [Os(1)–Os(3) 2.816(1) vs. 2.785(1) Å and Os(2)–Os(3) 2.832(1) vs. 2.797(1) Å] as a consequence of the electronic saturation of the cluster.

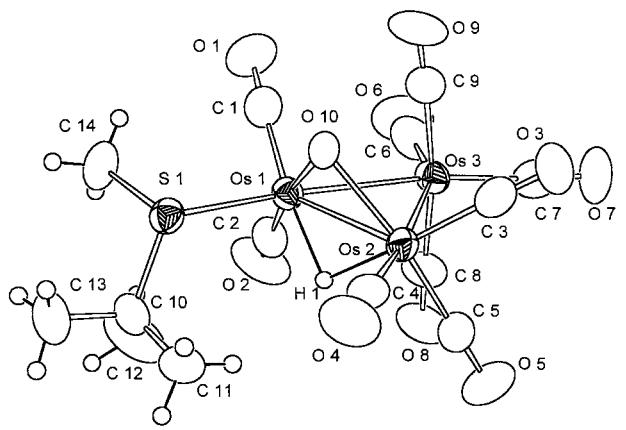

Fig. 5. An ORTEP plot of the molecular structure $[Os_3(CO)_9(\mu\text{-}H)(\mu\text{-}OH)(SMe^tBu)]$ **13**, showing the atom labelling scheme. Thermal ellipsoids are drawn at the 30% probability level.

Table 5
Selected bond lengths (Å) and angles (°) for $[Os_3(CO)_9(\mu\text{-}H)(\mu\text{-}OH)\{SMe(Bu^t)\}]$ (**11**)

Bond lengths			
Os(1)–Os(2)	2.809(1)	C(3)–O(3)	1.14(2)
Os(1)–Os(3)	2.816(1)	Os(2)–C(4)	1.94(1)
Os(2)–Os(3)	2.832(1)	C(4)–O(4)	1.12(1)
O(10)–Os(1)	2.146(7)	Os(2)–C(5)	1.88(1)
O(10)–Os(2)	2.142(7)	C(5)–O(5)	1.13(1)
S(1)–Os(1)	2.438(3)	Os(3)–C(6)	1.95(2)
S(1)–C(10)	1.89(1)	C(6)–O(6)	1.12(2)
S(1)–C(14)	1.80(1)	Os(3)–C(7)	1.93(2)
Os(1)–C(1)	1.89(2)	C(7)–O(7)	1.12(2)
C(1)–O(1)	1.15(2)	Os(3)–C(8)	1.93(1)
Os(1)–C(2)	1.86(1)	C(8)–O(8)	1.14(2)
C(2)–O(2)	1.12(2)	Os(3)–C(9)	1.95(1)
Os(2)–C(3)	1.92(2)	C(9)–O(9)	1.13(1)
Bond angles			
Os(2)–Os(1)–Os(3)	60.44(2)	C(5)–Os(2)–O(10)	169.5(4)
C(1)–Os(1)–C(2)	88.3(6)	C(3)–Os(2)–Os(1)	133.0(4)
C(1)–Os(1)–H(1)	173(3)	C(3)–Os(2)–Os(3)	87.3(4)
C(1)–Os(1)–O(10)	98.8(4)	C(4)–Os(2)–Os(1)	114.7(4)
C(1)–Os(1)–S(1)	98.0(4)	C(4)–Os(2)–Os(3)	174.2(4)
C(2)–Os(1)–H(1)	91(2)	C(5)–Os(2)–Os(1)	120.8(4)
C(2)–Os(1)–O(10)	171.2(4)	C(5)–Os(2)–Os(3)	93.7(4)
C(2)–Os(1)–S(1)	99.1(4)	H(1)–Os(2)–Os(1)	40.3(6)
S(1)–Os(1)–H(1)	90(3)	H(1)–Os(2)–Os(3)	81(3)
S(1)–Os(1)–O(10)	85.1(2)	O(10)–Os(2)–Os(1)	49.1(2)
S(1)–Os(1)–Os(2)	106.32(7)	O(10)–Os(2)–Os(3)	83.4(2)
S(1)–Os(1)–Os(3)	166.51(7)	Os(1)–Os(3)–Os(2)	59.66(2)
C(1)–Os(1)–Os(2)	136.0(4)	C(6)–Os(3)–C(7)	100.8(6)
C(1)–Os(1)–Os(3)	91.2(4)	C(6)–Os(3)–C(8)	91.4(6)
C(2)–Os(1)–Os(2)	122.2(4)	C(6)–Os(3)–C(9)	94.7(6)
C(2)–Os(1)–Os(3)	91.0(4)	C(7)–Os(3)–C(8)	93.4(6)
H(1)–Os(1)–Os(2)	40.3(6)	C(7)–Os(3)–C(9)	94.8(6)
H(1)–Os(1)–Os(3)	81(3)	C(8)–Os(3)–C(9)	168.7(5)
O(10)–Os(1)–Os(2)	49.0(2)	C(6)–Os(3)–Os(1)	98.0(4)
O(10)–Os(1)–Os(3)	83.7(2)	C(6)–Os(3)–Os(2)	157.6(4)
Os(1)–Os(2)–Os(3)	59.90(2)	C(7)–Os(3)–Os(1)	161.2(4)
C(3)–Os(2)–C(4)	95.8(5)	C(7)–Os(3)–Os(2)	101.6(4)
C(3)–Os(2)–C(5)	91.5(5)	C(8)–Os(3)–Os(1)	86.3(4)
C(3)–Os(2)–H(1)	168(3)	C(8)–Os(3)–Os(2)	85.3(4)
C(3)–Os(2)–O(10)	98.4(4)	C(9)–Os(3)–Os(1)	83.4(4)
C(4)–Os(2)–C(5)	91.1(5)	C(9)–Os(3)–Os(2)	85.4(3)
C(4)–Os(2)–H(1)	96(3)	C(10)–S(1)–C(14)	103.1(6)
C(4)–Os(2)–O(10)	91.3(4)	C(10)–S(1)–Os(1)	116.0(4)
C(5)–Os(2)–H(1)	88(2)	C(14)–S(1)–Os(1)	106.8(4)

3. Conclusions

In the present study, reaction of $[Os_3(CO)_{11}(NCMe)]$ with thioethers leads in all cases examined to the for-

mation of $[Os_3(CO)_{11}(L)]$ (L = thioether), albeit in moderate yield. The thioethers are coordinated in an equatorial site of the triosmium framework and there is no evidence for other coordination modes. On the other hand, the outcome of reactions of $[Os_3(CO)_{10}(NCMe)_2]$ with thioethers is less predictable and the factors governing product formation in these reactions require further detailed studies. For some thioethers, we observe formation of monosubstituted clusters in relatively high yield while other thioethers yield disubstituted clusters; no examples of clusters of the type $[Os_3(CO)_{10}(\mu\text{-}SR_2)]$ could be obtained in this investigation. Thioethers with aryl substituents undergo oxidative addition of a C–H bond of an aryl ring when reacted with $[Os_3(CO)_{10}(NCMe)_2]$ (cf. Scheme 1).

Reaction of (electrophilic) $[Os_3(\mu\text{-}H)_2(CO)_{10}]$ with the thioethers used in this work did not lead to discernable products except when trimethylamine N-oxide was added to the reaction mixture; in this case, clusters of the type $[Os_3(\mu\text{-}H)_2(CO)_9(L)]$ (L = thioether) were obtained. The fact that the thioethers used in this study do not add to the electrophilic dihydride cluster indicates that they are relatively weak nucleophiles. All new clusters reported here have been isolated in one form only; with the exception of enantiomeric forms, no isomers could be detected in solution or the solid state. While correlations have been made between stereoelectronic parameters (ligand cone angles and/or σ-donor strengths) and reactivity trends in associative substitution reactions of complexes of late transition metals [26,27,35], no correlation between these properties and the observed ligand coordination modes could be observed for the clusters discussed here. Attempts to achieve carbon-sulfur bond cleavage of the coordinated thioethers in compounds **1**–**10** through thermolysis with or without the presence of hydrogen gas are currently being undertaken (cf. [36]).

4. Experimental

All manipulations were carried out under an inert atmosphere of nitrogen using standard Schlenck and vacuum line techniques. The starting materials $[Os_3(CO)_{12}]$ [37] and $[Os_3(\mu\text{-}H)_2(CO)_{10}]$ [38] were prepared by published methods. Solvents were freshly distilled from appropriate drying agents. Thin layer chromatography (TLC) was carried out on commercial plates precoated with Merck Kieselgel 60 to 0.5 mm thickness. Infrared spectra were recorded on a Nicolet Avatar FT-IR spectrometer, ^{1}H-NMR spectra on a Varian Unity 300 MHz spectrometer using the solvent resonance as an internal standard, and FAB MS (3-nitrobenzyl alcohol matrix) on a JEOL SX-102 mass spectrometer.

4.1. Synthesis of $[Os_3(CO)_{11}(SEt_2)]$ (1)

Diethyl sulfide (15 μl, 0.14 mmol) was added by syringe to a solution of $[Os_3(CO)_{11}(NCMe)]$ (100 mg, 0.11 mmol) in CH_2Cl_2 (30 ml) and the mixture was stirred under nitrogen for 3 h at room temperature. Removal of the solvent under reduced pressure and TLC workup, using dichloromethane-hexane (3:7 v/v) as eluent gave $[Os_3(CO)_{11}(SEt_2)]$ **1**, yellow, (32 mg, 30%). Repeating the reaction using $[Os_3(CO)_{10}(NCMe)_2]$ as starting material and a longer reaction time (5 h), but otherwise identical reaction conditions, gave **1** in a higher yield (50 mg, 48%).

$[Os_3(CO)_{11}(SEt_2)]$ **1**: IR (cm^{-1}, CH_2Cl_2): ν(CO) 2108w, 2054vs, 2036m, 2017s, 1987sh, 1971m. ^{1}H-NMR ($CDCl_3$) δ (ppm): 2.91 (q, SCH_2CH_3), 1.32 (t, SCH_2CH_3). MS [FAB+, m/z]: 970 (M^+), M^+-^{n}CO ($n = 1$–11).

4.2. Synthesis of $[Os_3(CO)_{11}(SPr_2)]$ (2)

Di-*n*-propyl sulfide (20 μl, 0.14 mmol) was added by syringe to a solution of $[Os_3(CO)_{11}(NCMe)]$ (100 mg, 0.11 mmol) in CH_2Cl_2 (25 ml) and the mixture was stirred under nitrogen for 4–5 h at room temperature. Removal of the solvent under reduced pressure and TLC purification, using dichloromethane-hexane (1:1 v/v) as eluent, gave $[Os_3(CO)_{11}(SPr_2)]$ **2**, yellow, (37 mg, 29%). An identical reaction, using $[Os_3(CO)_{10}(NCMe)_2]$ as starting material, gave a higher yield of **2** (65 mg, 61%).

$[Os_3(CO)_{11}(SPr_2)]$ **2**: IR (cm^{-1}, CH_2Cl_2): ν(CO) 2108 w, 2054 s, 2034 s, 2017 vs, 1986 w, 1953 sh. ^{1}H-NMR ($CDCl_3$) δ (ppm): 2.93 (t, $SCH_2CH_2CH_3$), 1.7 (m, $SCH_2CH_2CH_3$), 1.05 (t, $SCH_2CH_2CH_3$). MS [FAB+, m/z]: 998 (M^+), (M^+-^{n}CO) $n = 1$–11.

4.3. Synthesis of $[Os_3(CO)_{11}\{SMe(Bu^t)\}]$ (3)

Methyl *tert*-butyl sulfide (18 μl, 0.14 mmol) was added by syringe to a solution of $[Os_3(CO)_{11}(NCMe)]$ (100 mg, 0.11 mmol) in CH_2Cl_2 (35 ml) and the mixture was stirred under nitrogen for 2 h at room temperature. Removal of the solvent under reduced pressure and TLC purification, using dichloromethane-hexane (1:1 v/v) as eluent, gave $[Os_3(CO)_{11}\{SMe(Bu^t)\}]$ **3**, yellow, (70 mg, 66%).

$[Os_3(CO)_{11}\{SMe(Bu^t)\}]$ **3**: IR (cm^{-1}, CH_2Cl_2): ν(CO) 2108w, 2054s, 2036m, 2018vs, 1986w, 1955sh. ^{1}H-NMR ($CDCl_3$) δ (ppm): 2.64 (s, $MeSBu^t$), 1.42 (s, $MeSBu^t$). MS [FAB+, m/z]: 984 (M^+), (M^+-^{n}CO) $n = 1$–11.

4.4. Reaction of $[Os_3(CO)_{10}(NCMe)_2]$ with $S(CH_2)_5$

This reaction is closely related to that reported by Adams *et al.* [19]. Pentamethylene sulfide (25 μl, 0.24

mmol) was added by syringe to a solution of $[Os_3(CO)_{10}(NCMe)_2]$ (100 mg, 0.11 mmol) in dichloromethane (20 ml) and the mixture was stirred under nitrogen at room temperature for 1 h. The solvent was removed under reduced pressure and the resulting residue was dissolved in a minimum amount of CH_2Cl_2 and applied to TLC plates. TLC using dichloromethane-hexane (1:1 v/v) as eluent gave two bands–in order of decreasing R_f, $[Os_3(CO)_{11}\{S(CH_2)_5\}]$ **4**, pale yellow (20 mg, 15%) and $[Os_3(CO)_{10}\{S(CH_2)_5\}_2]$ **5**, yellow (52 mg, 46%). The spectroscopic data for **4** and **5** were identical to those previously reported [19].

4.5. Synthesis of $[Os_3(\mu\text{-}H)(CO)_{10}(\mu\text{-}\eta^2\text{-}C_6H_4SPh)]$ (6) and $[Os_3(\mu\text{-}H)(CO)_9(\mu_3\text{-}C_6H_4SPh]$ (7)

Diphenyl sulfide (39 μl, 0.24 mmol) was added by syringe to a solution of $[Os_3(CO)_{10}(NCMe)_2]$ [100 mg, 0.11 mmol) in dichloromethane and the mixture was stirred under nitrogen at room temperature for 3 h. The solvent was removed under reduced pressure and the resulting residue was dissolved in a minimum amount of CH_2Cl_2 and purified by TLC plates using dichloromethane-hexane (1:4 v/v) as eluent. Three bands were recovered, in order of decreasing R_f: a yellow, as of yet uncharacterized product (trace), $[Os_3(\mu\text{-}H)(CO)_{10}(\mu\text{-}\eta^2\text{-}SC_6H_4Ph)]$ **6**, intense yellow, (46 mg, 41%) and $[Os_3(\mu\text{-}H)(CO)_9(\mu_3\text{-}C_6H_4SPh)]$ **6**, yellow (7 mg, 6.5%).

$[Os_3(\mu\text{-}H)(CO)_{10}(\mu\text{-}\eta^2\text{-}C_6H_4SPh)]$ **6**: IR (cm^{-1}, CH_2Cl_2): ν(CO) 2104s, 2064s, 2052s, 2021m, 2010m, 1992m, 1973sh. ^{1}H-NMR ($CDCl_3$) δ (ppm): 8.04 (d, 1H, JH-H = 7.7 Hz), 7.46–7.24 (m, S*Ph*), 6.92 (q, 2H), 6.74 (t, 1H), (−14.41) (s, Os(μ-H). MS [FAB+, m/z]: 1038(M^+), (M^+-^{n}CO) $n = 1$–10.

$[Os_3(\mu\text{-}H)(CO)_9(\mu_3\text{-}C_6H_4SPh)]$ **7**: IR (cm^{-1}, CH_2Cl_2): ν(CO) 2105m, 2076w, 2067s, 2024s. ^{1}H-NMR ($CDCl_3$) δ (ppm): 7.89 (d, C_6H_4SPh), 7.71–7.56 (m, C_6H_4S*Ph*), 7.36–7.22 (m, C_6H_4S*Ph*), 6.92 (t, C_6H_4SPh), 6.70 (t, C_6H_4SPh), 5.85 (d, C_6H_4SPh), (−14.85) (s, Os(μ-H)). MS [FAB+, m/z]: 1010 (M^+), (M^+-^{n}CO) $n = 1$–9.

4.6. Synthesis of $[Os_3(\mu\text{-}H)_2(CO)_9(SPr_2)]$ (8)

In a typical reaction, $[Os_3(\mu\text{-}H)_2(CO)_{10}]$ (100 mg, 0.12 mmol) and dipropyl sulfide (22 μl, 0.15 mmol) were mixed in CH_2Cl_2 (30 ml). To this solution, one equivalent of Me_3NO (12 mg, 0.15 mmol) in CH_2Cl_2 was added dropwise with a dropping funnel during one hour, and the resultant solution was stirred under nitrogen at room temperature for another 2 h, during which time a color change from purple to red was observed. The solvent was removed under reduced pressure and the resulting residue was dissolved in a minimum amount of CH_2Cl_2 and purified by TLC plates, using dichloromethane-hexane (1:4 v/v) as eluent. Two bands were recovered, in order of decreasing R_f: $[Os_3(\mu\text{-}H)_2(CO)_9(SPr_2)]$ **8**, red (34 mg, 31%) and a yellow, as of yet uncharacterised product (5 mg).

$[Os_3(\mu\text{-}H)_2(CO)_9(SPr_2)]$ **8**: IR (cm^{-1}, CH_2Cl_2): ν(CO) 2093s, 2054vs, 1010vs, 1990sh, 1941m. ^{1}H-NMR ($CDCl_3$) δ (ppm): 3.08 (t, SCH_2CH$_2$CH$_3$), 1.76 (m, SCH$_2$CH$_2$CH_3), 1.10 (t, SCH_2CH$_2$CH$_3$), (−10.0) (s, Os(μ-H)). MS [FAB+, m/z]: 944 (M^+).

4.7. Synthesis of $[Os_3(\mu\text{-}H)_2(CO)_9(SPh_2)]$ (9)

In a typical reaction, $[Os_3(\mu\text{-}H)_2(CO)_{10}]$ (100 mg, 0.12 mmol) and diphenyl sulfide (25 μl, 0.15 mmol) were mixed in CH_2Cl_2 (30 ml) and one equivalent of Me_3NO (12 mg, 0.15 mmol) in CH_2Cl_2 was added dropwise with a dropping funnel during one hour, and stirred under nitrogen at room temperature for 2 h. A color change from purple to red was observed. The solvent was removed under reduced pressure and the resulting residue dissolved in a minimum amount of CH_2Cl_2 and applied to TLC plates. TLC purification, using dichloromethane-hexane (1:4 v/v) as eluent, gave two bands, in order of decreasing R_f: $[Os_3(\mu\text{-}H)_2(CO)_9(SPh_2)]$ **9**, red (36 mg, 31%) and a yellow uncharacterized product (5 mg).

$[Os_3(\mu\text{-}H)_2(CO)_9(SPh_2)]$ **9**: IR [ν(CO) cm^{-1}, CH_2Cl_2]: 2096s, 2074w, 2058s, 2015s, 1993s, 1980m, 1953m. ^{1}H-NMR [δ (ppm), $CDCl_3$)]: 7.71–7.24 (m, S*Ph*$_2$), (−9.6) (s, Os(μ-H)). MS [FAB+, m/z]: 1012 (M^+).

4.8. Treatment of $[Os_3(\mu\text{-}H)_2(CO)_{10}]$ with $MeSBu^t$ and one equivalent Me_3NO

A total of 100 mg $[Os_3(\mu\text{-}H)_2(CO)_{10}]$ (0.12 mmol) and *tert*-butyl methyl sulfide (20 μl, 0.15 mmol) were mixed in CH_2Cl_2 (30 ml) and one equivalent of Me_3NO (12 mg, 0.15 mmol) in CH_2Cl_2 was added dropwise with a dropping funnel for 1 h, and stirred under nitrogen at room temperature for 4 h. A color change from purple to red was observed. The solvent was removed under reduced pressure and the resulting residue dissolved in a minimum amount of CH_2Cl_2 and applied to TLC plates, using dichloromethane–hexane (3:7 v/v) as eluent. Two bands were recovered: in order of decreasing R_f, $[Os_3(\mu\text{-}H)_2(CO)_9(SMeBu^t)]$ **10**, red, (56 mg, 53%) $[Os_3(\mu\text{-}H)(\mu\text{-}OH)(CO)_9(SMeBu^t)]$ **11**, yellow (16 mg, 15%) and a yellow, as of yet uncharacterized product (13 mg).

$[Os_3(\mu\text{-}H)_2(CO)_9(SMeBu^t)]$ **10**: IR [ν(CO) cm^{-1}, CH_2Cl_2]: 2096s, 2057vs, 2015vs, 2004s, 1991s, 1979m, 1947m. ^{1}H-NMR [δ (ppm), $CDCl_3$)]: 2.77 (s, *Me*SBu^t), 1.48 (s, MeS*Bu*^{t}), (−10.0) (s, Os(μ-H)). MS [FAB+, m/z]: 930 (M^+).

$[Os_3(\mu\text{-}H)(\mu\text{-}OH)(CO)_9(SMeBu^t)]$ **11**: IR [ν(CO) cm^{-1}, CH_2Cl_2]: 2099s, 2057vs, 2034vw, 2019s, 2015sh, 2002s, 1980m, 1975m, 1938m. ^{1}H-NMR [δ (ppm),

$CDCl_3$)]: 2.88 (s, *Me*SBu^t), 1.49 (s, MeS*Bu*^{t}), (− 12.3) (s, Os(μ-H)). MS [FAB + , *m*/*z*]: 946 (M^+).

4.9. X-ray data collection and structure determination of *1*, *2*, *4*, *10* and *11*

Crystal data and other experimental details for all structures are reported in Table 6. The diffraction experiments for compounds **1**, **2**, **4**, **10** were carried out on an Enraf-Nonius CAD4 diffractometer at room temperature, using graphite-monochromatized Mo–K_α radiation ($\lambda = 0.71073$ Å). The unit cells were determined by a least-squares fitting procedure using 25 randomly selected strong reflections. The diffracted intensities were corrected for Lorentz and polarization effects. An empirical absorption correction was applied using the azimuthal scan method [39]. The metal atom positions were determined by direct methods (SIR-97 [40]) and all non-hydrogen atoms were located from Fourier difference syntheses. In compound **10**, the two bridging hydrides were also located in the Fourier map. The methyl and methylene H atoms were added in calculated positions (d_{C-H} 0.98 and 0.95 Å, respectively). The final refinement on F^2 proceeded by full-matrix least-squares calculations (SHELX-93 [41]) using anisotropic thermal parameters for all the non-hydrogen atoms. The methyl and methylene hydrogen atoms were assigned an isotropic thermal parameters 1.5 times the U_{eq} values of the carrier carbon atoms. The relatively low quality of the diffraction data for compound **1** was due to the fact that good quality crystals could not be obtained despite repeated crystallizations by different techniques.

The X-ray intensity data for **11** were measured on a Bruker AXS SMART 2000 diffractometer, equipped with a CCD detector, using Mo–K_α radiation ($\lambda = 0.71073$ Å) at room temperature. Cell dimensions and the orientation matrix were initially determined from least-squares refinement on reflections measured in three sets of 20 exposures collected in three different ω regions and eventually refined against 3615 reflections. A full sphere of reciprocal space was scanned by 0.3° ω steps with the detector kept at 5.0 cm from the sample.

Table 6
Crystal data and experimental details for $[Os_3(CO)_{11}(SEt_2)]$ (**1**); $[Os_3(CO)_{11}(SPr_2)]$ (**2**); $[Os_3(CO)_{11}\{S(CH_2)_5\}]$ (**4**); $[Os_3(\mu\text{-}H)_2(CO)_9(SMeBu^t)]$ (**10**); $[Os_3(\mu\text{-}H)(\mu\text{-}OH)(CO)_9\{SMe(Bu^t)\}]$ (**11**)

Compound	**1**	**2**	**4**	**10**	**11**
Empirical formula	$C_{15}H_{10}O_{11}Os_3S_1$	$C_{17}H_{14}O_{11}Os_3S_1$	$C_{16}H_{10}O_{11}Os_3S_1$	$C_{14}H_{14}O_9Os_3S_1$	$C_{14}H_{14}O_{10}Os_3S_1$
Molecular weight	968.89	996.94	980.90	928.91	944.91
Temperature (K)	293(2)	293(2)	293(2)	298(2)	293(2)
Wavelength (Å)	0.71069	0.71069	0.71069	0.71069	0.71073
Crystal symmetry	Monoclinic	Triclinic	Monoclinic	Monoclinic	Monoclinic
Space group	$P2_1/n$ (No. 14)	$P\bar{1}$ (No. 2)	$P2_1/c$ (No. 14)	$P2_1/n$ (No. 14)	$C2/c$ (No. 15)
a (Å)	8.301(4)	9.538(3)	8.289(3)	10.207(6)	23.212(2)
b (Å)	16.323(4)	11.413(9)	9.568(3)	13.992(6)	8.853(1)
c (Å)	16.653(7)	12.828(4)	28.336(9)	15.285(7)	21.318(2)
α (°)	90	70.15(5)	90	90	90
β (°)	98.48(3)	109.47(3)	93.98(4)	91.05(4)	90.488(3)
γ (°)	90	108.29(5)	90	90	90
Cell volume (Å^3)	2232(2)	1206(1)	2239(1)	2183(2)	4308.8(6)
Z	4	2	4	4	8
D_{calc} (Mg m^{-3})	2.884	2.745	2.909	2.827	2.865
μ(Mo–K_α) (mm^{-1})	17.182	15.900	17.126	17.556	17.449
F(000)	1728	896	1752	1656	3376
Crystal size (mm)	0.15 × 0.22 × 0.35	0.25 × 0.28 × 0.35	0.05 × 0.12 × 0.40	0.10 × 0.15 × 0.25	0.25 × 0.30 × 0.35
θ limits (°)	2.60–29.98	2.25–30.17	2.25–24.98	2.38–25.07	1.75–30.16
Reflections collected	6492 ($\pm h$, $+k$, $+l$)	7361 ($\pm h$, $\pm k$, $+l$)	3450 ($\pm h$, $+k$, $+l$)	3981 ($\pm h$, $+k$, $+l$)	28864 ($\pm h$, $\pm k$, $\pm l$)
Unique observed reflections [$F_o > 4\sigma(F_o)$]	6492	7070	3379	3831	6454
Goodness-of-fit on F^2	1.029	1.056	1.083	1.066	0.875
$R_1(F)$ [a], $wR_2(F^2)$ [b]	0.0748, 0.1885	0.0503, 0.1321	0.0334, 0.0627	0.0302, 0.0822	0.0420, 0.0896
Weighting scheme	$a = 0.1554$, $b = 0.0000$ [b]	$a = 0.0762$, $b = 5.6460$ [b]	$a = 0.0226$, $b = 19.3098$ [b]	$a = 0.0592$, $b = 3.4393$ [b]	$a = 0.0452$, $b = 0.0000$ [b]
Largest difference peak and hole (e Å^{-3})	2.357 and −2.123	2.192 and −1.661	0.982 and −0.944	1.348 and −1.290	1.663 and −1.072

[a] $R_1 = \Sigma||F_o| - |F_c||/\Sigma|F_o|$.
[b] $wR_2 = [\Sigma w(F_o^2 - F_c^2)^2/\Sigma w(F_o^2)^2]^{1/2}$ where $w = 1/[\sigma^2(F_o^2) + (aP)^2 + bP]$ where $P = (F_o^2 + 2F_c^2)/3$.

Intensity decay was monitored by recollecting the initial 50 frames at the end of the data collection and analyzing the duplicate reflections. The collected frames were processed for integration by using the program SAINT and an empirical absorption correction was applied using SADABS [42] on the basis of the Laue symmetry of the reciprocal space. The structure was solved by direct methods (SIR-97) [40] and subsequent Fourier syntheses and refined by full-matrix-block least-squares on F^2 (SHELXTL) [43] using anisotropic thermal parameters for all non hydrogen atoms. The bridging hydride was located in the Fourier map and refined with a fixed isotropic thermal parameter.

5. Supplementary material

Observed and calculated mass spectra for compounds **1**–**11** (22 pages). Crystallographic data for the structural analyses have been deposited with the Cambridge Crystallographic Data Centre, CCDC No. 152932 for $[Os_3(CO)_{11}(SEt_2)]$ (**1**), No. 152933 for $[Os_3(CO)_{11}(SPr_2)]$ (**2**), No. 152934 for $Os_3(CO)_{11}\{S(CH_2)_5\}$ (**4**), No. 152935 for $[Os_3(CO)_9(\mu\text{-}H)_2\{SMe(Bu^t)\}]$ (**10**), and No. 152936 for $[Os_3(CO)_9(\mu\text{-}H)(\mu\text{-}OH)\{SMe(Bu^t)\}]$ (**11**). Copies of this information may be obtained from The Director, CCDC, 12 Union Road, Cambridge, CB2 1EZ, UK (Fax: +44-1223-336033; e-mail: deposit@ccdc.cam.ac.uk or www: http://www.ccdc.cam.ac.uk).

Acknowledgements

This research has been supported by grants to E.N. from the Swedish Natural Science Research Council (NFR) and the Swedish Engineering Sciences Research Council (TFR) and by grants from the Consiglio Nazionale delle Ricerche (CNR), MURST (COFIN98) and the University of Bologna ('Funds for Selected Research Topics') to M.M.

References

[1] H. Topsøe, B.S. Clausen, F.E. Massoth, in: J.R. Anderson, M. Boudart (Eds.), Hydrotreating Catalysis, Catalysis-Science and Technology, vol. 11, Springer-Verlag, Berlin, 1996.
[2] B.C Wiegand, C.M Friend, Chem. Rev. 92 (1992) 491.
[3] M. Monari, R. Pfeiffer, U. Rudsander, E. Nordlander, Inorg. Chim. Acta 247 (1996) 131.
[4] K. Kiriakidou, M.R. Plutino, F. Prestopino, M. Monari, L.I. Elding, E. Valls, R. Gobetto, S. Aime, E. Nordlander, Chem. Commun. (1998) 2721.
[5] N.K. Kiriakidou-Kazemifar, M. Haukka, T.A. Pakkanen, S.P. Tunik, E. Nordlander, J. Organomet. Chem. 623 (2001) 65.
[6] S. Rossi, J. Pursiainen, M. Ahlgren, T.A. Pakkanen, Organometallics 9 (1990) 475.
[7] S. Rossi, J. Pursiainen, T.A. Pakkanen, Organometallics 10 (1991) 1390.
[8] S. Rossi, K. Kallinen, J. Pursiainen, T.T. Pakkanen, T.A. Pakkanen, J. Organomet. Chem. 419 (1991) 219.
[9] R.D. Adams, R.A. Katahira, L.-W. Yang, Organometallics 1 (1982) 235.
[10] W.R. Cullen, S.J. Rettig, T.C. Zheng, Polyhedron 14 (2000) 2653.
[11] R.D Adams, S.B Fallon, Chem. Rev. 95 (1995) 2587.
[12] R.D. Adams, Aldrichim. Acta 33 (2000) 39.
[13] R.D. Adams, J.A. Belinski, J. Cluster Sci. 1 (1990) 319.
[14] R.D Adams, M.P Pompeo, J. Am. Chem. Soc. 113 (1991) 1619.
[15] R.D. Adams, J.E. Cortopassi, S.B. Fallon, Organometallics 11 (1992) 3794.
[16] R.D. Adams, J.A. Belinski, Organometallics 11 (1992) 2488.
[17] R.D. Adams, M.P. Pompeo, Organometallics 11 (1992) 2281.
[18] R.D Adams, M.P. Pompeo, W. Wu, J.H. Yamamoto, J. Am. Chem. Soc. 115 (1993) 8207.
[19] R.D. Adams, J.E. Cortopassi, J.H. Yamamoto, W. Wu, Organometallics 12 (1993) 4955.
[20] M.R. Churchill, B.G. Deboer, Inorg. Chem. 16 (1977) 878.
[21] R.D. Adams, I.T. Horvath, B.E. Segmüller, L.-Y. Yang, Organometallics 2 (1983) 144.
[22] A.J. Deeming, S. Donovan-Mtunzi, S.E. Kabir, P.J. Manning, J. Chem. Soc. Dalton Trans. (1985) 1037.
[23] R.D. Adams, X. Qu, W. Wu, Organometallics 12 (1993) 4117.
[24] S. Aime, R. Gobetto, E. Valls, Inorg. Chim. Acta 275 (1998) 521.
[25] E. Nordlander, B.F.G. Johnson, J. Lewis, P.R. Raithby, J. Chem. Soc. Dalton Trans. (1996) 3825.
[26] T. Shi, L.I. Elding, Inorg. Chem. 35 (1996) 5941.
[27] A.A. Tracey, K. Eriks, A. Prock, W.P. Giering, Organometallics 9 (1990) 1399.
[28] R.E. Benfield, B.F.G. Johnson, J. Lewis, P.R. Raithby, C. Zuccaro, K. Henrick, Acta Crystallogr. Sect. B B35 (1979) 2210.
[29] (a) M.R. Churchill, F.J. Hollander, J.P. Hutchinson, Inorg. Chem. 16 (1977). (b) V.F. Allen, R. Mason, P.B. Hitchcock, J. Organomet. Chem. 140 (1977) 297. (c) A. Guy Orpen, A. Valentina Rivera, E.G. Bryan, D. Pippard, G.M. Sheldrick, J. Chem. Soc. Chem. Commun. (1978) 723. (d) R.W. Broach, J.M. Williams, Inorg. Chem. 18 (1979) 314.
[30] R.D. Adams, B.E. Segmuller, Cryst. Struct. Commun. 11 (1982) 1971.
[31] L.J. Farrugia, J. Organomet. Chem. 394 (1990) 515.
[32] R.D. Adams, N.M. Golembeski, Inorg. Chem. 18 (1979) 1909.
[33] L. Heuer, E. Nordlander, B.F.G. Johnson, J. Lewis, P.R. Raithby, Phosphorus, Sulfur and Silicon 103 (1995) 241.
[34] D.W. Knoeppel, J-H. Chung, S.G. Shore, Acta Crystallogr. Sect. B 51 (1995) 42.
[35] L. Chen, A.J. Poë, Coord. Chem. Rev. 143 (1995) 265.
[36] R.D. Adams, O-S. Kwon, J.L. Perrin, Organometallics 19 (2000) 2246.
[37] B.F.G. Johnson, J. Lewis, Inorg. Synth. 13 (1972) 93.
[38] (a) A.J. Deeming, S. Hasso, M. Underhill, J. Chem. Soc. Dalton Trans. (1975) 1614. (b) H.D. Kaesz, S.A.R. Knox, J. Koepke, R. Saillant, J. Chem. Soc. Chem. Commun. (1971) 477. (c) B.F.G. Johnson, J. Lewis, P. Kilty, J. Chem. Soc. Sect. A. (1965) 2859.
[39] A.C.T. North, D.C. Philips, F.S. Mathews, Acta Crystallogr. Sect A 24 (1968) 351.
[40] A. Altomare, M.C. Burla, M. Camalli, G.L. Cascarano, C. Giacovazzo, A. Guagliardi, A.G.G. Moliterni, G. Polidori, R. Spagna, J. Appl. Cryst. 32 (1999) 115.
[41] G.M. Sheldrick, SHELXL-93, Program for crystal structure refinement, University of Göttingen, Germany, 1993.
[42] G.M. Sheldrick, SADABS, program for empirical absorption correction, University of Göttingen, Germany, 1996.
[43] G.M. Sheldrick, SHELXTLPLUS Version 5.1 (Windows NT version) Structure Determination Package; Bruker Analytical X-ray Instruments Inc. Madison, WI, 1998.